UDC621.313.8

AXIAL-FLUX PERMAMENT MAGNET MACHINE WITH REDUCED CONSUMPTION OF ACTIVE MATERIALS

E. Monakhov, V. Chumack
National Technical University of Ukraine "Kyiv Polytechnic Institute"
ul. Politechnicheskaya, 37, korp. 20, Kyiv, 03056, Ukraine
E-mail: emonachov@gmail.com; chumack_kpi@ukr.net

This article deals with one-sided axial-flux permanent magnet generator with reduced consumption of active materials, particularly permanent magnets. This research compares conventional design of electric machine and design which have the same quantity of pole pairs, but half of them are replaced by steel cores. Comparison was made with help of three-dimensional field model built in ANSYS Maxwell 3D FEM environment. Model validity was proved by experiments. Experiments were carried out using manufactured axial-flux permanent magnet generator. Error is about 10 % that is satisfactory due to the absence of input control of active materials. Proposed design was optimized by parametric optimization in order to eliminate the non-uniformity of induction in the air gap. Also, as conclusions, article gives some recommendations about proposed design of axial-flux permanent magnet generator.

Key words: axial-flux, generator, permanent magnet, active material, simulations.

ТОРЦЕВА МАГНІТОЕЛЕКТРИЧНА МАШИНА ЗІ ЗНИЖЕНИМИ ВИТРАТАМИ АКТИВНИХ МАТЕРІАЛІВ

Є. А. Монахов, В. В. Чумак
Національний технічний університет України «Київський політехнічний інститут»
вул. Політехнічна, 37, корп. 20, м. Київ, 03056, Україна
E-mail: emonachov@gmail.com; chumack_kpi@ukr.net

Розглянуто конструкцію торцевої односторонньої магнітоелектричної машини зі зниженими витратами активних матеріалів, зокрема, постійних магнітів. Дослідження проводилось із застосуванням польової тривимірної моделі. Проведено порівняння машини традиційної конструкції з числом магнітів, що дорівнює кількості пар полюсів, і машини запропонованої конструкції, але із заміною половини постійних магнітів на стальні осердя. Порівняння проводилось на основі тривимірних польових моделей, побудованих на базі програмного забезпечення ANSYS Maxwell. Достовірність моделі підтверджено випробуваннями, й похибка складає порядку 10 %, що є задовільним за умови відсутності вхідного контролю активних матеріалів. Експерименти проводились на виготовленому торцевому магнітоелектричному генераторі. Запропонована конструкція була оптимізована за допомогою параметричної оптимізації з метою усунення нерівномірності індукції у повітряному проміжку. Надано рекомендації щодо запропонованої конструкції.

Ключові слова: торцевий, генератор, постійні магніти, активні матеріали, моделювання.

PROBLEM STATEMENT. Every year spread of permanent magnet electric machines in different scopes increases [1, 2]. Last decade of years axial-flux permanent magnet generators have developed in small and medium-scale power generation systems, mostly wind turbines and small hydropower plants [3, 4].

Permanent magnet synchronous generators are more attractive than induction machines in terms of cost and performance [5, 6].

Axial-flux permanent magnet machines have some advantages over radial-flux electric machines with permanent magnets [7]. They may be designed with higher power–to–weight ratio, which results into decreasing of using the active materials [8, 9]. Also axial flux machines have planar air gap, which may be adjustable.

The most expensive and important part of every permanent magnet generator is surely permanent magnet. There are two main permanent magnets used in machinery: NdFeB and SmCo. Their characteristics and comparison are shown below in table 1.

Table 1 – Comparison of characteristics of permanent magnet

Type of magnet	Br, kG	Hc, kOe	BHmax, MGOe
NdFeB	10.6…14.5	10.4…12.7	28…52
$SmCo_5$	8.6…11.6	8.2…10.8	18…32

Rare earth permanent magnet NdFeB has the highest energy characteristic, but it has lower temperature stability than SmCo. In some cases when electric machine or apparatus operates under conditions with increased temperature, the latter magnet can be applied. Between 150 K and 150 °C out performs NdFeB for flux output. Above 150 °C NdFeB suffers sufficient loss in induction that SmCo is superior. Where induction must be stable over a wide temperature range, SmCo is superior [10].

Table 2 presents comparisons of magnet and system costs and weight of permanent magnets made by Arnold Magnetic Technologies [10]. All results were calculated at 23 °C.

Table 2 – Comparisons of magnet and system costs and weight

Material	BHmax, MGOe	Magnet Material	Relative cost of magnet in System	Total System	Relative system weight
NdFeB 38 SH (sintered)	37.8	20	2.7	1.0	1.0
Ferrite (sintered)	3.9	1	1.0	1.1	1.5
SmCo 28 (sintered)	28.8	28	5.5	1.3	1.0
NdFeB (Inj molded)	6.4	23	13.7	2.2	1.3
NdFeB (Comp bonded)	10.5	23	9.1	1.7	1.2

"Magnet Material" refers to the relative cost per pound. "Magnet in the System" refers to the cost of the weight of magnet used in the system. For example, less NdFeB would be used than ferrite for equivalent output. Therefore, the "Magnet in the System" NdFeB cost is relatively closer to Ferrite. Any model has limitations and should be used wisely. Wherever there are questions a knowledgeable applications engineer should be consulted. Also this model is suitable for simple geometry magnets. Where shape complexity occurs, it may be necessary to use a bonded magnet or one that is easier to magnetize in a complicated pattern, such as ferrite. In almost every case, it is impossible simply substitute one material for another. Substitution requires a re-design, a change both in the soft magnetic return path and in the copper (electric circuit). This model does not consider assembly costs. It does consider most of the required design changes related to different materials. The model demonstrates that for many applications NdFeB is now fully price competitive with ferrite.

Bonded Magnets have greater shape flexibility and may be made into very complex structures.

As it is shown, the choice of permanent magnet plays the most important role. Permanent magnets of SmCo type are the most expensive.

This article deals with a construction of axial-flux permanent magnet generator with reduced consumption of active material, particularly, permanent magnets [11, 12]. Proposed design is shown in Fig. 1.

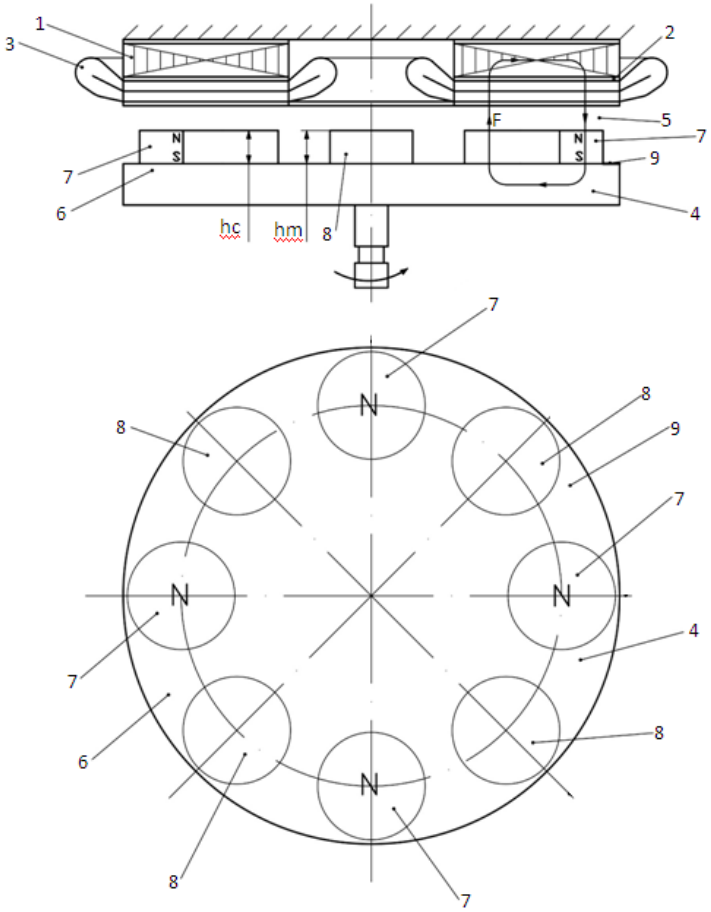

Figure 1 – General view of axial-flux permanent magnet generator:
1 – core; 2 – slots; 3 – winding; 4 – rotor; 5 – air gap; 6 – ferromagnetic disk; 7 – permanent magnets; 8 – steel cores; 9 – surface of a disk

This design differs from conventional by quantity of used permanent magnets. Half of pole pairs are replaced by steel cores, number of which are twice less than number of pole pairs. Cores are located symmetrically on a circle between the permanent magnets. At the same time permanent magnets have same polarity relatively to disk. Flux F closes the next magnetic path: magnet 7 – disk 6 – ledge 8 – air gap 5 – stator yoke 1 – air gap 5 – permanent magnet 7. While rotor 4 is rotating, electromotive force is being induced in winding 3. It is a generator mode of axial-flux permanent magnet machine.

This construction was mentioned in work [11] of native engineer and scientist Palastin, but wasn't investigated.

This design was investigated by finite element method. The field model was created in ANSYS Maxwell.

Fig. 2 shows a three-dimensional model of conventional axial-flux permanent magnet generator in ANSYS Maxwell.

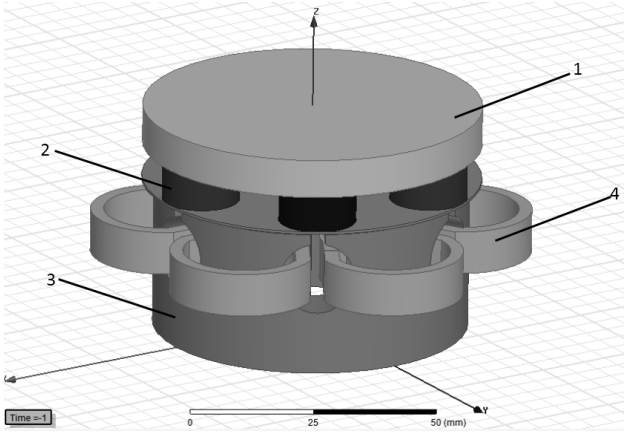

Figure 2 – 3D model of axial – flux permanent magnet generator:
1 – rotor; 2 – permanent magnets; 3 – stator;
4 – winding

Input data for simulation are shown in table 3.

Table 3 – Input data for model

Parameter	Value
Permanent magnets	NdFeB N38H: B_r=1,21 Tesla, H_c=939 kA/m
Material of rotor	Steel 3
Material of stator	Steel 1211
Turns in the coil	110
Angular velocity	1000 rpm
Number of pole pairs	6

In the calculation of the magnetic field it was used transient nonlinear differential equation for the magnetic vector potential (A) which moves in conductive medium [13].

$$\vec{\nabla}\times\frac{1}{\mu}\,\vec{\nabla}\times\vec{A}\,-\gamma\frac{\partial\vec{A}}{\partial t}+\gamma\vec{V}\times\,\vec{\nabla}\times\vec{A}\,=-\vec{J}\,,$$

where μ, γ – magnetic permeability and electrical conductivity respectively; $\vec{V}$ $\vec{J}$ – vector of velocity motion of the medium and current density vector; $\vec{\nabla}$ – differentional nabla operator (Del).

A following assumptions were taken into account during simulation:

1) losses due to eddy current effects in active parts of electrical machines weren't took into an account;

2) the stator is made massive;

3) the winding of the stator represented as single-turn. It partitioned in the computation domain into real number of turns W.

Boundary conditions. On the surface of computational domain according to Dirichlet boundary condition the value of the function specified below:

$$A\big|_G = 0.$$

On the external borders of the computational domain the conditions for the continuity of the field vectors are set.

Initial conditions. Initial conditions are necessary for solving the time-dependent nonstationary analysis. It is necessary to set the initial conditions – values of the field function in the middle of the field at the initial time:

$$A(x,y,z,t)\big|_{t=0} = A(x,y,z,0)\,.$$

Result of field simulation is shown in Fig. 3.

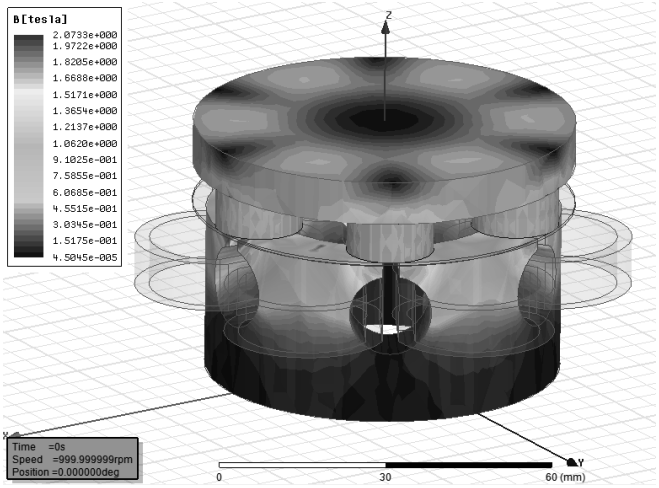

Figure 3 – Results of 3D simulation

Maximum value of induction is about 2 Tesla in the crown of teeth. Also external characteristic of conventional axial-flux permanent magnet generator was calculated. External characteristic of generator is shown in Fig. 4.

EXPERIMENTAL PART AND RESULTS OBTAINED. Relevance of 3D field model was confirmed by experiments. There was designed and manufactured an axial-flux permanent magnet generator (Fig. 5).

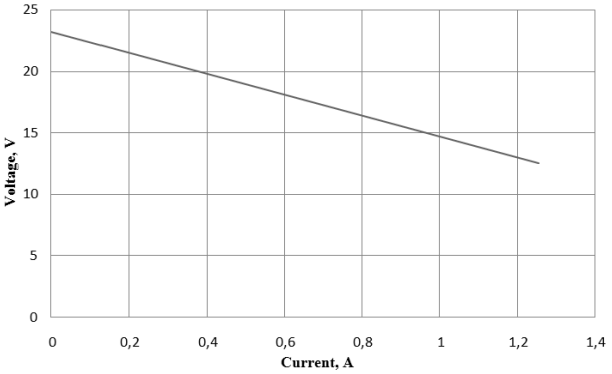

Figure 4 – External characteristic of generator

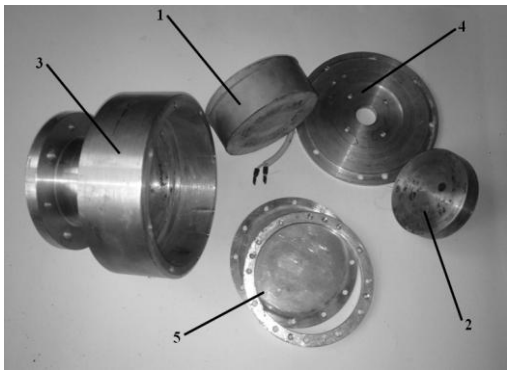

Figure 5 – Disassembled axial-flux permanent magnet generator: 1 – stator; 2 – rotor; 3 – case; 4 – mounting disk for stator; 5 – structural elements

There were 2 stages of check up.

Stage 1. Ohmic resistance was measured and compared with the magnetostatic simulation results in Maxwell. Table 4 shows comparison of measured and computed resistance.

Table 4 – Comparison of measured and computed resistance

	Computed	Experiment	Error, %
Resistance, ohm	5.814	6.1	4.68 %

The value of error is less than 10 % that shows a good conformity of model and manufactured generator.

Stage 2. External characteristic of generator was taken experimentally. It is shown in Fig. 6. Also Fig. 6 shows the computed external characteristic for a comparison. The load is active.

To sum up, the 3D dimensional model is correct and adequate to manufactured real generator.

After a confirmation of three-dimensional model developed in ANSYS Maxwell a model for research of proposed design was created. The difference between two models is that a half of magnets are replaced by steel cores. The same material as for rotor was chosen (Steel 3) for steel cores.

The simulation result of proposed design is shown in Fig. 7.

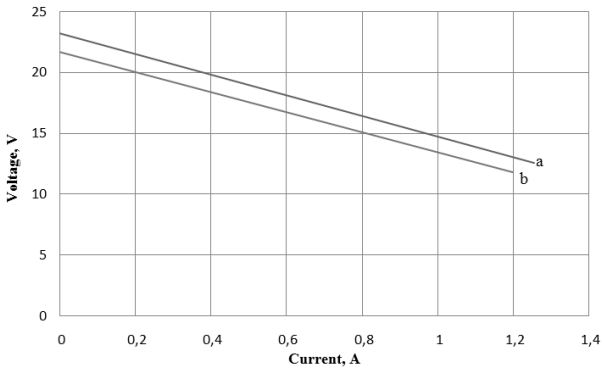

Figure 6 – External characteristic of generator: a – simulation; b – experiment

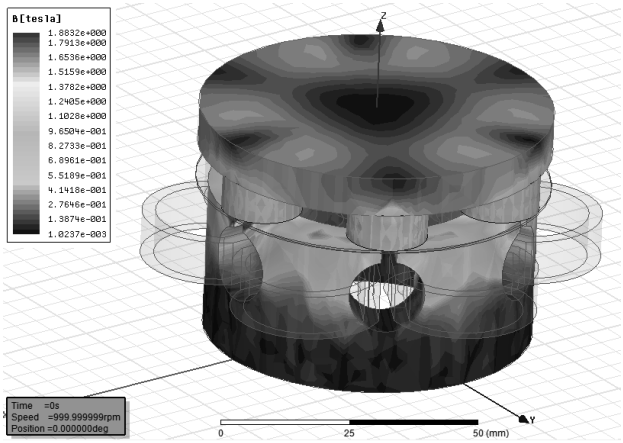

Figure 7 – Results of 3D simulation of proposed generator

Maximum value of induction is about 1.88 Tesla in the crown of teeth. It is seen that average value of induction in air gap is decreased. External characteristic was computed and shown in Fig. 8. Also at the same Fig. 8 it is shown simulated external characteristic of conventional axial gap permanent magnet generator for comparison.

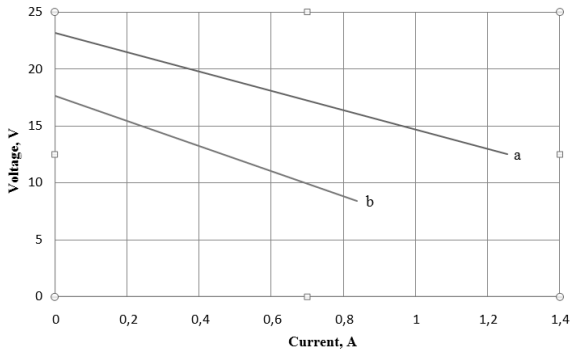

Figure 8 – Simulated external characteristic of axial-flux permanent magnet generator

It is seen that second characteristic (b) of proposed design lies lower than for traditional design. It is seen that voltage drop at operating mode is 4.17 V (it is about 17.9 %). Current drop is 0.41 A that is about 33.2 %.

It should be mentioned that induction in air gap between permanent magnet and stator differs from the induction between steel core and stator. The distribution of induction per one pole pair is shown in Fig. 9.

It is seen that value of induction under the cores is less than under the permanent magnet. Replacement of half of magnets by steel cores led to displacement of the operating point of the magnet.

In Fig. 10 it is shown operating point of magnet before replacement the half of magnets.

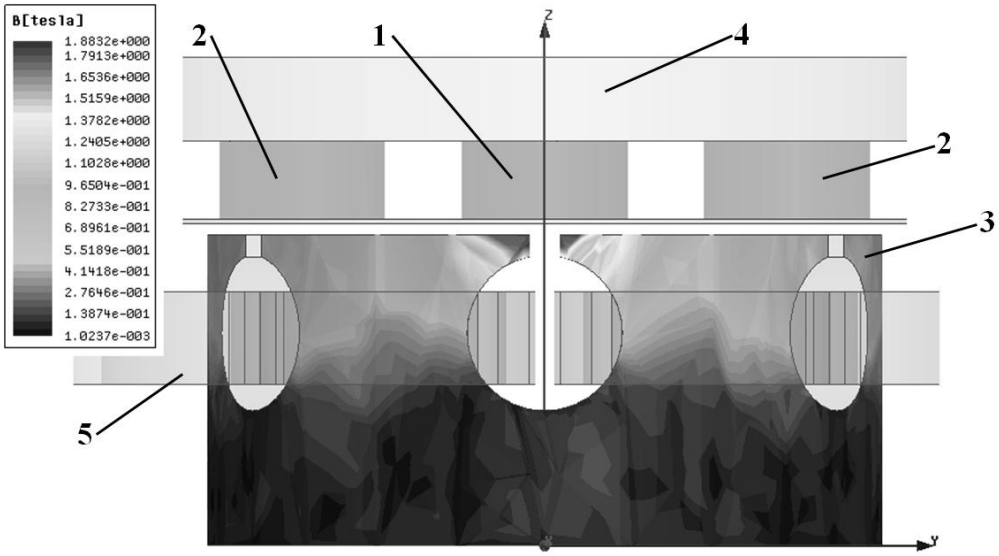

Figure 9 – Distribution of induction in the stator:
1 – permanent magnet; 2 – steel core; 3 – stator; 4 – rotor; 5 – winding

.

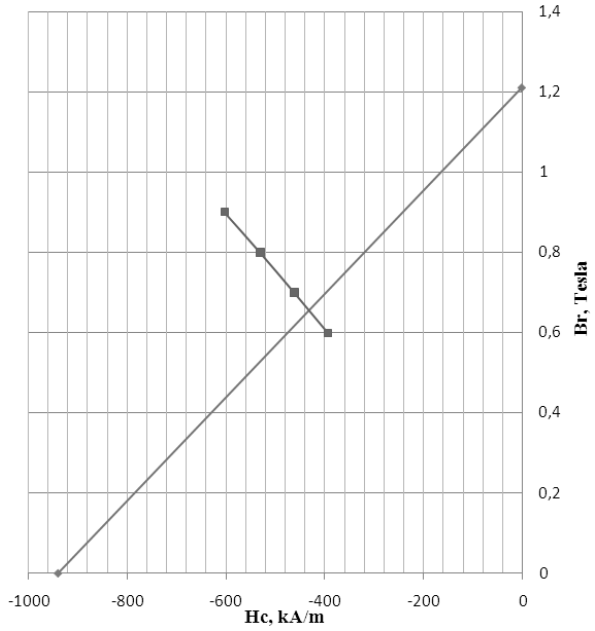

Figure 10 – Operating point of the magnet before replacement

Operating point of the magnet has following parameters:

B_{m0}=0.661 Tesla, H_c=435 kA/m.

Operating point was calculated by methods described in [14, 15]. In Fig. 11 it is shown new operating point of the magnet after replacement a half of magnets by steel cores.

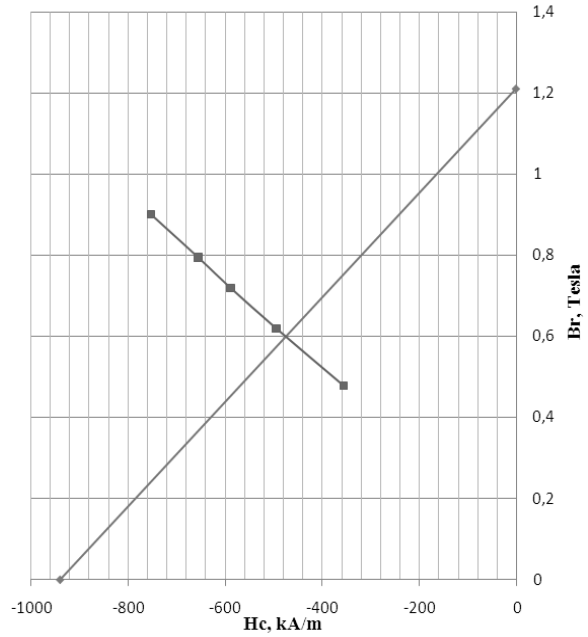

Figure 11 – Operating point of the magnet after replacement

Operating point of the magnet after replacement the half of magnets by steel cores has following parameters:

B_{m0}=0,56Tesla, H_c=480 kA/m.

In order to eliminate the unevenness of induction in the air gap it have to be changed either the cross section of the cores or the cross section of permanent magnets, or both of them.

It is necessary to make parametric or optimization calculation for selection of the optimal value of the cross section.

Parametric calculation was provided by ANSYS Maxwell. Parametric calculation was carried out in the following range:

$$S_{min} = 78\ mm^2 \text{ to } S_{max} = 315\ mm^2 .$$

Results of parameterization are shown as a dependence of open circuit voltage from the area of the core. The obtained results are shown in Fig. 12.

The scatter of curve points (Fig. 12,a) is caused by the lack of accuracy and not enough dense mesh that has been set in the simulation. Curve shown in Fig. 12,a was interpolated and shown in Fig. 12,b. Voltage differs from its minimum value of 17.06 V to 17.9 V.

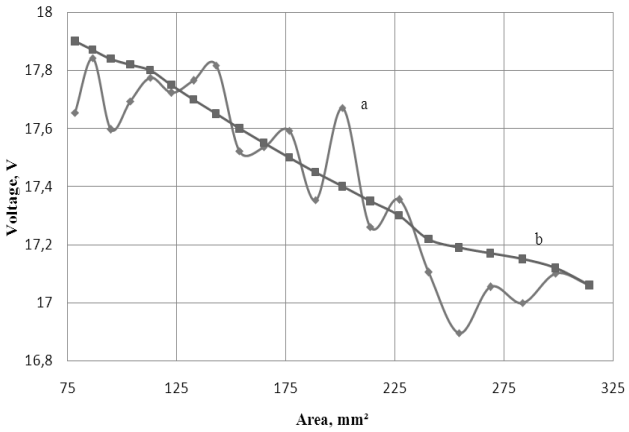

Figure 12 – Dependence U=*f*(Score)
a – simulated dependence; b – interpolated results

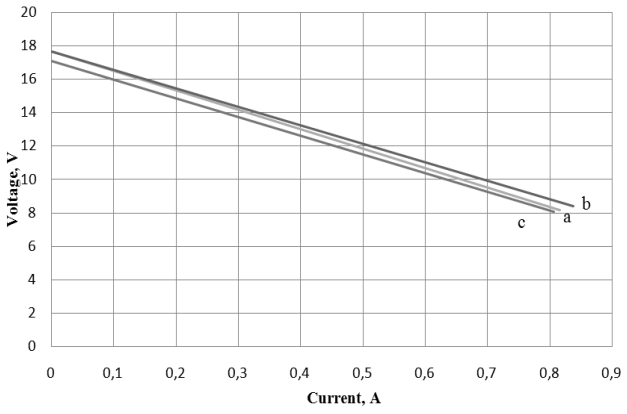

Figure 13 – Comparison of simulated characteristics
a = 16mm, b =20 mm, c = 10 mm

It is seen that the change the value of cross section and volume of steel cores didn't let to the desired result. In figure 13 it is shown comparison of a few simulated external characteristic with different cross section of magnet. It means that change of the area of magnetic steel cores is not enough to eliminate the unevenness of induction in the air gap and to level up external characteristic. Elimination of the unevenness of induction in air gap and leveling up the characteristic is probably possible by setting a flux concentrator and changing the magnetic circuit of the inductor of axial- flux permanent magnet generator.

CONCLUSIONS. It this work three-dimensional model of axial-flux permanent magnet was developed. It's relevance was checked up by the experiments. Experiments confirmed the adequacy of the three-dimensional model.

Purposed design allows one to create machine with reduced consumption of active material with saving the number of pore pairs.

As it was expected, energy density felt proportionally to the total volume of magnets. However, this design allows one to create machines with double quantity of poles. If, for example, required double frequency compared with the frequency of the drive mechanism, proposed design may solve this issue.

REFERENCES

1. Jacek, F. Gieras, Rong-Jie, Wang and Maarten, J. Kamper (2008), Axial Flux Permanent Magnet Brushless Machines, Springer, USA.

2. Bannon, Nick, Davis, Jimmy and Clement, Erin (2013), Axial flux permanent magnet generator, University of Washington, USA.

3. Chalmers, B.J. and Spooner, E. (1999), "An axial-flux permanent-magnet generator for a gearless wind energy system", *Energy Conversion*, *IEEE Transactions*, vol. 14, no. 2, pp. 251–257.

4. Holmes, Andres S., Hong, Guodong and Pullen, Keith R. (2005), "Axial flux permanent magnet micro power generation", *Journal of micro electromechanical systems*, Vol. 4, no. 1, pp. 54–62.

5. Bumby, J. and Martin, R. (2005), "Axial-flux permanent-magnet air-cored generator for small-scale wind turbines", *IEE Proceedings, Electric Power Applications*, Vol. 5, pp. 1065–1075.

6. Howey, D.A. (2009), Axial flux permanent magnet generators for pico-hydropower, *EWB-UK Research Conference, Electrical Engineering Department*, Imperial College, United Kingdom.

7. Rabinovich, R. (1996), "Magnetic field analysis of permanent magnet motors", *IEEE Transactionson magnetic*, Vol. 32, no. 1, pp. 265–269.

8. Meo, S. and Esposito, F. (2007), "Suite for the computer-aided analysis of advanced automotive electrical power system", *International Review of Electrical Engineering (IREE)*, Vol. 2, no. 6, pp. 751–762.

9. Zhang, D., Chau, K.T., Niu S. and Jiang, J.Z. (2006), "Design and analysis of a double-stator cup rotor PM integrated-starter-generator", *IEEE IAS Annual Meeting*, pp. 20–26.

10. Constantinides, Steve (2012), Material Matters, *Arnold magnetic technologies*.

11. Palastin, M. (1980), *Sinkhronnye mashiny avtonomnykh istochnikov pitaniya* [Synchronous machines for autonomous energy sources], Energia, Moscow. (in Russian)

12. Application for a patent № u2014 12948.

13. Vaskovskiy, Y.M. (2007), *Polyovyi analiz elektychnykh mashyn* [Field analysis of electrical machines], NTUU "KPI", Kyiv. (in Ukrainian)

14. Kaftanatiy, V. (2014), "Theoretical research and calculation of onephase micro generator for robotics", *Energia – XXI*, no. 1, 2, pp. 116–130.

15. Shishkin, V. (2006), *Avtomatizirovannoe proektirovanie torcovykh magnitoehlektricheskikh generatorov peremennogo toka* [Computer-aided design of axial-flux permanent magnet alternative generators], Ivanovo Power Engineering Institute named after V.I. Lenin, Ivanovo. (in Russian)

ТОРЦЕВАЯ МАГНИТОЭЛЕКТРИЧЕСКАЯ МАШИНА С УМЕНЬШЕННЫМ РАСХОДОМ АКТИВНЫХ МАТЕРИАЛОВ

Е. А. Монахов, В. В. Чумак

Национальный технический университет Украины «Киевский политехнический институт»

ул. Политехническая, 37, корп. 20, г. Киев, 03056, Украина.

E-mail: emonachov@gmail.com; chumack_kpi@ukr.net

Рассмотрена конструкция торцевой односторонней магнитоэлектрической машины со сниженным расходом активных материалов, в частности, постоянных магнитов. Исследование проводилось с применением полевой трехмерной модели. Проведено сравнение машины традиционной конструкции с числом магнитов, равным числу пар полюсов, и машины предложенной конструкции с таким же числом пар полюсов, но с заменой половины постоянных магнитов на стальные сердечники. Сравнение производилось с помощью трехмерных полевых моделей, построенных на базе программного обеспечения ANSYS Maxwell. Достоверность модели подтверждена испытаниями, и погрешность составляет порядка 10 %, что является удовлетворительным по причине отсутствия входного контроля активных материалов. Эксперименты проводились на изготовленном торцевом магнитоэлектрическом генераторе. Предложенная конструкция была оптимизирована с помощью параметрической оптимизации с целью устранения неравномерности индукции в воздушном зазоре. Даны рекомендации относительно предложенной конструкции.

Ключевые слова: торцевой, генератор, постоянные магниты, активные материалы, моделирование.

Стаття надійшла 12.05.2015.